Finite-size effect in the Schwinger particle-production mechanism

Ren-Chuan Wang*
Oak Ridge National Laboratory and Joint Institue for Heavy-Ion Research, Oak Ridge, Tennessee 37831 and Texas A&M University, College Station, Texas 77843

Cheuk-Yin Wong
Oak Ridge National Laboratory, Oak Ridge, Tennessee 37831
(Received 11 January 1988)

The Schwinger mechanism of particle production in a strong and uniform electric field for an infinite system is generalized to the case where the strong field is confined between two condenser plates separated by a finite distance. The production rates, for both bosons and fermions, are obtained by solving the Klein-Gordon equation and the Dirac equation in a linear vector potential. They are expressed in terms of parabolic cylinder functions for bosons, and in terms of the confluent hypergeometric functions for fermions. Numerical evaluation of these results shows large deviations of the production rate from what one deduces with the Schwinger formula, indicating a large finite-size effect in particle production.

I. INTRODUCTION

The Schwinger mechanism of pair production,[1] first put forth to examine the production of electron-positron pairs in a strong and uniform electric field, has been applied to many problems in contemporary physics.[2-7] Many different derivations of the Schwinger results have been put forth.[8-11] In the physics of black holes, the Schwinger mechanism has been invoked to understand Hawking's predictions of black-hole quantum evaporation.[2,12] If one assumes that the wave function is analytic near the horizon, then the spectrum of created particles as obtained by such a mechanism is consistent with Hawking's thermodynamical interpretation of the properties of a temperature and a physical entropy.[2] In the physics of macroscopic electronic circuits, the effect of particle production is hindered by the small size of the transition energy as compared to barrier height which is of the order of the electron mass. There is a recent suggestion of using the resistively shunted Josephson junction to lower the barrier height through quantum fluctuations to allow the occurrence of pair production.[6]

The Schwinger mechanism has often been invoked to study particle production in QCD (Refs. 3–5, 9, and 10). As applied to nucleon-nucleon or e^+-e^- collisions, the field between a quark and an antiquark is represented, as an approximation, by an Abelian gauge field, in the same form as the constant electric field between two condenser plates in quantum electrodynamics (QED). Particles are produced when a quark from the negative-energy sea tunnels through a barrier and emerges as a quark in positive-energy states. Such an application has met a high degree of success. In particular, one can explain qualitatively the falloff of the transverse momentum of the produced particles, the suppression of the strangeness and baryon production, the K/π ratio[3] and the time delay in particle production after a collision takes place. Recently, with the advent of relativistic heavy-ion beams, there is much interest in the particle-production mechanism in nuclear collisions[5,13-19] which is a complicated problem in quantum chromodynamics (QCD). The Schwinger mechanism has been used to study some aspects of possible collision scenarios.[18,19]

Because of the various applications of the Schwinger mechanism, it is worthwhile to reexamine the basis of the Schwinger results and the domain of their applicability. We note that the original case considered by Schwinger is for a uniform electric field extending to all regions of space, in contrast with the situation where for many applications the linear potential fields are often finite in extent. Here, we wish to consider the case where the strong field is confined between two condenser plates separated by a finite distance. We would like to examine how the finite spatial separation affects the pair-production rate. We expect that in line with similar problems in quantum physics, the rate of particle production will show a finite-size effect which will manifest itself as large fluctuations and deviations from the Schwinger results when the separation between the plates becomes small. This problem of condenser plates with a finite separation may also be useful to provide an understanding of the time delay in particle production observed in nuclear collisions.[13,14]

We shall treat the case of both bosons and fermions in a strong linear vector potential between two parallel plates separated by a distance L. The original treatment of Schwinger for an infinite system made use of the Green's function and its behavior under gauge transformations. We shall use an alternative approach here by solving the single-particle Klein-Gordon and the Dirac equations. In Sec. II we study the problem of bosons in a linear vector potential bounded by two parallel plates. We solve the Klein-Gordon equation and obtain the solution for the region between the plates in terms of the parabolic cylinder functions.[20] The transmission amplitude for an incoming negative-energy state is then obtained by matching the wave functions at the boundaries. In Sec.

III we study the same problem of a fermion in a linear vector potential between two plates. The fermion case for particles with no transverse momentum was solved previously.[21] We shall study here the more general case including the transverse-momentum degree of freedom with a slightly simpler method. The solutions of the Dirac equation for the incoming negative-energy states are expressed in terms of confluent hypergeometric functions with complex arguments and parameters. The transmission amplitude is obtained by matching the wave functions at the boundaries. In Sec. IV we discuss how the transmission amplitude is related to the pair-production rate. We compare our results with Schwinger's and show how the two results agree at the midpoint between the plates when the separation becomes very large. A correction to the Schwinger formula for particle production at this midpoint is obtained. Using the pair-production process in QCD as an illustrative case, we give numerical results for particle-production rates as a function of the coordinates between the plates in Sec. V. As expected, however, for finite separations, the deviations of the numerical results from Schwinger's results are large. Section VI concludes the present discussion.

II. BOSONS IN A LINEAR VECTOR POTENTIAL

We consider a boson with a mass m in a static linear vector potential $A=(0, A_0(z))$ of the form [Fig. 1(a)]

$$A_0=\begin{cases}0 & \text{for } z\le 0 \text{ (region I)}\ ,\\ -\kappa z & \text{for } 0\le z\le L \text{ (region II)}\ ,\\ -\kappa L & \text{for } L\le z \text{ (region III)}\ .\end{cases} \tag{2.1}$$

Such a potential arises, for example, for charged bosons in the electric field of two parallel condenser plates separated by a distance L. The strength parameter κ of the vector potential is then related to the charge of the particle e and the electric field $\mathcal{E}$ by $\kappa=|e\mathcal{E}|$. It also arises in an approximate treatment of particle production in QCD. When a pair of quarks and an antiquark $q\bar{q}$ are stretched, the field between the quark and the antiquark is represented as an approximation by an Abelian gauge field. The strength parameter κ is then related to the string tension.[3] The case of fermions will be studied in the next section. We examine here the Klein-Gordon equation ($\hbar=c=1$) for the particle given by

$$[(p-A)^2-m^2]\phi=0\ . \tag{2.2}$$

The potential does not depend on the transverse coordinates x and y. The wave function in the transverse coordinates is just a plane wave with transverse momentum $\mathbf{p}_T=(p_x,p_y)$. The solution of the Klein-Gordon equation can be written in the form

$$\phi=\exp[i(p_x x+p_y y-Et)]f(z)\ , \tag{2.3}$$

where E is the energy of the state under consideration. We make the transformation from z to a dimensionless length ξ:

$$\xi=\sqrt{2}(E+\kappa z)/\sqrt{\kappa}\ . \tag{2.4}$$

The corresponding dimensionless length coordinate ξ_L for the left condenser plate at $z=0$ becomes

$$\xi_L=\sqrt{2}E/\sqrt{\kappa} \tag{2.5}$$

and the dimensionless length coordinate for the right condenser plate at $z=L$ becomes

$$\xi_R=\sqrt{2}(E+\kappa L)/\sqrt{\kappa}\ . \tag{2.6}$$

The solutions of Eq. (2.2) in regions I and III are just plane waves. We need only to find the solutions of Eq. (2.2) in region II. In this region and in terms of the dimensionless length coordinates, Eq. (2.2) becomes the following Schrödinger-type equation:

$$\left[-\frac{d^2}{d\xi^2}+a-\tfrac{1}{4}\xi^2\right]f(\xi)=0\ , \tag{2.7}$$

where

$$a=\frac{m_1^2}{2\kappa}=\frac{m^2+\mathbf{p}_T^2}{2\kappa}\ . \tag{2.8}$$

The Schrödinger-type equation is formally the same as that for an effective potential $V_{\text{eff}}(\xi)$ of an inverted para-

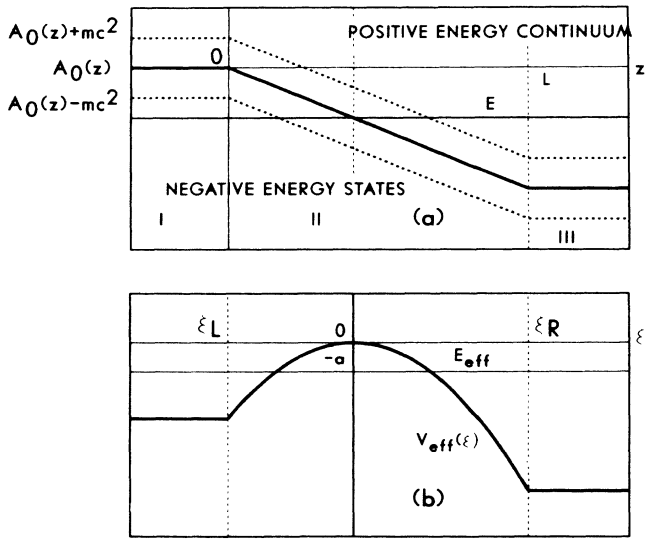

FIG. 1. In (a) the solid curve shows the linear vector potential in region II (between $0<z<L$) and the constant potential in region I ($z<0$) and region III ($z>L$). The upper-dashed curve shows the location of the vector potential plus the rest mass $A_0(z)+mc^2$, above which lies the positive continuum, and the lower-dashed curve shows the location of the vector potential minus the rest mass $A_0(z)-mc^2$, below which lies the negative continuum. In (b) the Klein-Gordon or the Dirac equation for the potential of (a) is rewritten in a Schrödinger-type form in terms of dimensionless coordinate ξ, and the linear vector potential of (a) then gives rise to an effective potential of an inverted parabola with an effective energy $E_{\text{eff}}=-a$ for the Klein-Gordon case and $E_{\text{eff}}=-a\pm i/2$ for the Dirac case. The top of the barrier in (b) is located at the coordinate corresponding to the point at which $E=A_0(z)$ in (a). A negative-energy state in region I can tunnel through the barrier and be transmitted as a positive-energy state in region III.

bola $-\frac{1}{4}\xi^2$ which is joined to $-\frac{1}{4}\xi_L^2$ on the left at ξ_L, and joined onto $-\frac{1}{4}\xi_R^2$ on the right at ξ_R [Fig. 1(b)]. We note that the transverse momentum provides an additional effective mass which must work against the strong field for a tunneling event to occur. Thus, with this additional contribution, the rest mass becomes the "transverse mass" $m_\perp=(m^2+\mathbf{p}_T^2)^{1/2}$. The effective energy E_{eff} in this inverted parabola problem is then $-a$. In this region of an inverted parabola (region II), the solutions of Eq. (2.7) are well known.[22] They are the parabolic cylinder functions $E(a,\xi)$ and $E^*(a,\xi)$ (Ref. 20). Tunneling is possible if

$$-a \geq -\xi_L^2/4 \quad \text{and} \quad -a \geq -\xi_R^2/4 \ . \tag{2.9}$$

These conditions imply that tunneling can take place only when

$$L \geq 2m_\perp/\kappa \tag{2.10}$$

and

$$-m_\perp \geq E \geq -\kappa L + m_\perp \ . \tag{2.11}$$

Thus, there is a separation threshold $2m_\perp/\kappa$ below which no particle will be produced. This minimum separation is proportional to the transverse mass $m_\perp$ and inversely proportional to the strength of the field κ. We shall solve the Schrödinger-type equation (2.7) for states within this limit of Eq. (2.11), appropriate for incoming negative-energy states with an energy $E<0$ incident to region I from the left ($z=-\infty$) and are transmitted as positive-energy states with energy $(E+\kappa L)>0$ propagating to the right ($z=+\infty$). We shall label the wave function of one such state $n(\xi)$ where n stands for a negative-energy state in region I. The solution of Eq. (2.2) is

$$\begin{aligned}
&\text{region I,} \quad n_1(\xi)=Ia_I e^{-ik_L\xi}+Ra_R e^{+ik_L\xi} \ ; \\
&\text{region II,} \quad n_2(\xi)=AE(a,\xi)+BE^*(a,\xi) \ ; \\
&\text{region III,} \quad n_3(\xi)=Ta_T e^{+ik_R\xi} \ ;
\end{aligned} \tag{2.12}$$

where

$$k_{L,R}=(\tfrac{1}{4}\xi_{L,R}^2-a)^{1/2} \tag{2.13}$$

and the functions $E(a,\xi)$ and $E^*(a,\xi)$ are parabolic cylinder functions[20] which should not be confused with the energy E. The constants a_I, a_R, and a_T are normalization constants such that incident, reflected, or transmitted plane waves φ_i and φ_j with momenta $\mathbf{p}_i$ and $\mathbf{p}_j$ and energies E_i and E_j in the asymptotically free regions are orthonormalized according to[23]

$$\begin{aligned}
(\varphi_i,\varphi_j)&\equiv\int d^3r\frac{i}{2}[\varphi_i^*\partial_t\varphi_j-(\partial_t\varphi_i^*)\varphi_j] \\
&=\delta(\mathbf{p}_i-\mathbf{p}_j)E_i/|E_i| \ .
\end{aligned} \tag{2.14}$$

Explicitly, the normalization constants are

$$a_I=a_R=1/|E|^{1/2} \quad \text{and} \quad a_T=1/|E+\kappa L|^{1/2} \ . \tag{2.15}$$

Note that the velocity of the incident wave in region I represented by $e^{-ik_L\xi}$ points to the positive z direction, even though the current propagates to the opposite direction because the energy E and the density are negative. We set the amplitude I to be unity to obtain T as the transmission amplitude and R as the reflection amplitude. After matching the wave functions and their derivatives at the boundary points ξ_L and ξ_R, we obtain the transmission amplitude T as given by

$$T=\frac{a_I}{a_T}\frac{4k_L\exp[i(k_L\xi_L-k_R\xi_R)]}{(E_L'-ik_LE_L)(E_R^{*\prime}-ik_RE_R^*)-(E_L^{*\prime}-ik_LE_L^*)(E_R'-ik_RE_R)} \ , \tag{2.16}$$

where we have abbreviated

$$E_{L,R}=E(a,\xi_{L,R}) \quad \text{and} \quad E_{L,R}'=dE(a,\xi)/d\xi \ \text{at} \ \xi=\xi_{L,R} \ . \tag{2.17}$$

The reflection amplitude R is

$$R=\frac{a_I}{a_R}\exp(-ik_L\xi_L-ik_R\xi_R)\frac{(E_L'+ik_LE_L)(E_R^{*\prime}-ik_RE_R^*)-(E_L^{*\prime}+ik_LE_L^*)(E_R'-ik_RE_R)}{(E_L'-ik_LE_L)(E_R^{*\prime}-ik_RE_R^*)-(E_L^{*\prime}-ik_LE_L^*)(E_R'-ik_RE_R)} \ . \tag{2.18}$$

In the above equation, the factor (a_I/a_R) is equal to unity. They are retained here to show the similarity of the results for bosons and fermions in a later comparison [with Eq. (3.21) below].

With the wave functions as given in Eqs. (2.3) and (2.12), we can obtain the incident, reflected, and transmitted currents as follows:

$$\begin{aligned}
&\mathbf{J}_I=\mathbf{p}_I I^*I/|E| \ , \\
&\mathbf{J}_R=\mathbf{p}_R R^*R/|E| \ , \\
&\mathbf{J}_T=\mathbf{p}_T T^*T/|E+\kappa L| \ ,
\end{aligned} \tag{2.19}$$

where

$$\mathbf{p}_I=(p_x,p_y,-\sqrt{2\kappa}k_L), \ \mathbf{p}_R=(p_x,p_y,\sqrt{2\kappa}k_L) \ ,$$

and

$$\mathbf{p}_T=(p_x,p_y,\sqrt{2\kappa}k_R) \ .$$

From Eqs. (2.14) and (2.16), we can use the properties of the parabolic cylinder function[20] to obtain the relationship

$$|R|^2=1+\left|\frac{k_RE}{k_LE'}\right||T|^2 \ , \tag{2.20}$$

where $E'=E+\kappa L$ is the energy of the particle in the transmitted region (region III) and should not be confused with the derivative of parabolic cylinder function $E'(a,\xi)$. We note that the ratio $|k_R E/k_L E'|$ is equal to the ratio of the speed of the particle in the z direction in region III to the speed of the particle in the z direction in region I. From Eq. (2.19) we see that Eq. (2.20) expresses the conservation of current in the z direction, i.e.,

$$(\mathbf{J}_I+\mathbf{J}_R)\cdot\mathbf{e}_z=\mathbf{J}_T\cdot\mathbf{e}_z \ . \tag{2.21}$$

III. FERMIONS IN A LINEAR VECTOR POTENTIAL

The results in the last section have been obtained for bosons. For fermions, we need to solve the corresponding Dirac equation. This can be carried out in the same way as in Ref. 21 with some modifications. We consider a fermion with a mass in a static linear vector potential $A=(0, A_0(z))$ as given in the previous case by Eq. (2.1) and shown in Fig. 1(a). The Dirac equation for the fermion (in the notation and convention of Bjørken and Drell, Ref. 24) is

$$[\gamma^\mu(p_\mu-A_\mu)-m]\psi=0 \ . \tag{3.1}$$

We introduce a spin function φ to write the solution of the Dirac equation ψ in the form

$$\psi=[\gamma^\mu(p_\mu-A_\mu)+m]\phi \ , \tag{3.2}$$

the Dirac equation then becomes

$$[(p-A)^2-m^2-i\sigma^{\mu\nu}(p_\mu-A_\mu)(p_\nu-A_\nu)]\phi=0 \ . \tag{3.3}$$

With the vector field as given by Eq. (2.1), Eq. (3.3) becomes

$$[(p-A)^2-m^2-i\kappa\alpha_3]\phi=0 \ . \tag{3.4}$$

As in the boson case, the wave function in the transverse coordinates is just a plane wave with transverse momentum $\mathbf{p}_\perp=(p_x,p_y)$. The solution of the Dirac equation can be written in the form

$$\phi=\exp[i(p_x x+p_y y-Et)]n(z) \ . \tag{3.5}$$

We expand the wave function in terms of the components f_λ and spinor μ_λ as

$$n(z)=\sum_{\lambda=1}^{4} f_\lambda(z)\mu_\lambda \ , \tag{3.6}$$

where

$$\mu_1=\frac{1}{\sqrt{2}}\begin{bmatrix}1\\0\\1\\0\end{bmatrix}, \quad \mu_2=\frac{1}{\sqrt{2}}\begin{bmatrix}0\\1\\0\\-1\end{bmatrix},$$

$$\mu_3=\frac{1}{\sqrt{2}}\begin{bmatrix}1\\0\\-1\\0\end{bmatrix}, \quad \text{and } \mu_4=\frac{1}{\sqrt{2}}\begin{bmatrix}0\\1\\0\\1\end{bmatrix} .$$

These spinor states μ_λ are chosen to be diagonal in α_3:

$$\alpha_3\mu_\lambda=\eta\mu_\lambda \ , \tag{3.7}$$

where the eigenvalues of α_3 are

$$\eta=+1 \text{ for } \lambda=1,2 \text{ and } \eta=-1 \text{ for } \lambda=3,4 \ .$$

To write down the solutions of the Dirac equation, we make the transformation from z to a dimensionless length ξ:

$$\xi=\sqrt{2}(E+\kappa z)/\sqrt{\kappa} \ . \tag{3.8}$$

The solutions in regions I and III are just plane waves. We only need to find the solutions in region II. For region II ($0<z<L$), the Dirac equation (3.4) becomes the Schrödinger-type equation

$$\left[-\frac{d^2}{d\xi^2}+\left[a+\eta\frac{i}{2}\right]-\tfrac{1}{4}\xi^2\right]f_\lambda(\xi)=0 \ , \tag{3.9}$$

where the quantity a is defined as before by Eq. (2.8). Equation (3.9) is in the same form as Eq. (2.7) for the boson case, except that the term a for bosons now becomes the complex quantity $\alpha=a+\eta i/2$ for fermions. Similar to the boson case, the Schrödinger-type equation for fermions is formally the same as that for a potential of an inverted parabola $V_{\text{eff}}(\xi)-\frac{1}{4}\xi^2$ which is joined to $-\frac{1}{4}\xi_L^2$ on the left at ξ_L and joined to $-\frac{1}{4}\xi_R^2$ on the right at ξ_R [Fig. 1(b)]. For the fermion case, the effective energy E_{eff} in this inverted parabola problem is then $-\alpha=-(a+\eta i/2)$. In this region of an inverted parabola (region II), although the solutions of Eq. (3.9) with a complex parameter α can be formally written in terms of the parabolic cylinder functions, there are no tables and numerical procedures for their evaluation. It is more convenient to write down the solutions in terms of the confluent hypergeometric function ${}_1F_1$ (Ref. 20). The two independent solutions for f_λ for $\lambda=1$ and 2 are

$$M(a,\xi)=\exp(i\xi^2/4)\,{}_1F_1\left[\frac{a}{2}i,\frac{1}{2},-\frac{i}{2}\xi^2\right] \tag{3.10}$$

and

$$N(a,\xi)=\xi\exp(i\xi^2/4)\,{}_1F_1\left[\frac{1+ai}{2},\frac{3}{2},-\frac{i}{2}\xi^2\right] . \tag{3.11}$$

For $\lambda=3$ and 4, the two independent solutions are $M^*(a,\xi)$ and $N^*(a,\xi)$. We shall solve the Schrödinger-type equation (3.9) for an incoming negative-energy state with an energy $E<0$ incident to region I from the left at $z=-\infty$ and is transmitted as a positive-energy state with an energy $E'=E+\kappa L>0$ to the right at $z=+\infty$. We shall label the wave function of one such a state as $n(\xi)$, where n stands for a negative-energy state in the asymptotic region I. The wave functions for regions I and III are given as follows:

$$\text{region I,} \quad n_1(\xi)=Ie^{-ik_L\xi}\chi_I+Re^{+ik_L\xi}\chi_R \ , \tag{3.12}$$

$$\text{region III,} \quad n_3(\xi)=Te^{+ik_R\xi}\chi_T \ , \tag{3.13}$$

where $k_{L,R}$ are defined as before, and I, R, and T are the

coefficients for the incident, reflected, and transmitted waves, respectively. The χ-spinors χ_K are given by

$$\chi_K = a_K(\gamma \cdot p_K + m)\mu_\lambda, \quad K = I, R, \text{ and } T , \tag{3.14}$$

where a_K are normalization constants such that $\chi_K^\dagger \chi_K$ is normalized to unity and the four-momenta in Eq. (3.14) for regions I and III are

$$\begin{aligned} p_I &= (E, p_x, p_y, -p_z) , \\ p_R &= (E, p_x, p_y, p_z) , \\ p_T &= (E', p_x, p_y, p_z') \end{aligned} \tag{3.15}$$

with $p_z = \sqrt{2\kappa} k_L$ and

$$p_z' = (E'^2 - m^2 - p_x^2 - p_y^2)^{1/2} = \sqrt{2\kappa} k_R .$$

The quantities p_z and p_z' in Eq. (3.15) are chosen to be positive so that the currents associated with the incident wave and the transmitted wave propagate to the right along the z axis, and the reflected wave propagates to the left opposite to the direction of the z axis. With these choices, the signs of the exponential factor $k\xi$ in the various terms of Eqs. (3.12) and (3.13) are then obtained as indicated. In terms of the momenta, the normalization constants are

$$\begin{aligned} a_I &= [2E(E + p_z)]^{-1/2} , \\ a_R &= [2E(E - p_z)]^{-1/2} , \end{aligned} \tag{3.16}$$

and

$$a_T = [2E'(E' - p_z')]^{-1/2} .$$

The solution in region II ($0 < z < L$) is given by

$$n_2(\xi) = \left[\gamma^0(E + \kappa z) - (\gamma^1 p_x + \gamma^2 p_y) + i\gamma^3 \frac{d}{dz} + m \right] \times [AM(a,\xi) + BN(a,\xi)]\mu_\lambda , \tag{3.17}$$

where A and B are complex coefficients and the first factor of operators on the right-hand side is to ensure that $n_2(\xi)$ satisfies the Dirac equation.

From Eq. (3.4), we observe that spinors with different components of λ are decoupled from one another. A solution of the wave function can be characterized by a single component of λ and by an eigenvalue η [Eq. (3.7)].

The coefficient of the incident wave I can be taken to be unity without much loss of generality. The unknown coefficients can be obtained by matching the wave functions at the boundaries. The boundary conditions for the Dirac equation are that the spinor wave functions are continuous across the boundary at $z=0$ and L. When these conditions are explicitly written out, they involve the Dirac γ matrices. We can consider first the case of $\lambda = 1$ and 2. From the independence of the γ matrices, one finds that the matching conditions have the same form as those of the boson case except that the function $E(a,\xi)$ has been replaced by $M(a,\xi)$ and the other independent function $E^*(a,\xi)$ has been replaced by $N(a,\xi)$. In consequence, the transmission coefficient T for fermions is

$$T = \frac{a_I}{a_T} \frac{4k_L \exp[i(k_L\xi_L - k_R\xi_R)]}{(M_L' - ik_L M_L)(N_R' - ik_R N_R) - (N_L' - ik_L N_L)(M_R' - ik_R M_R)} , \tag{3.18}$$

where we have abbreviated

$$M_{L,R} = M(a, \xi_{L,R}), \quad M_{L,R}' = dM(a,\xi)/d\xi \text{ at } \xi = \xi_{L,R} , \tag{3.19}$$

$$N_{L,R} = N(a, \xi_{L,R}), \quad N_{L,R}' = dN(a,\xi)/d\xi \text{ at } \xi = \xi_{L,R} . \tag{3.20}$$

The reflection amplitude R is

$$R = \frac{a_I}{a_R} \exp(-ik_L\xi_L - ik_R\xi_R) \frac{(M_L' + ik_L M_L)(N_R' - ik_R N_R) - (N_L' + ik_L N_L)(M_R' - ik_R M_R)}{(M_L' - ik_L M_L)(N_R' - ik_R N_R) - (N_L' - ik_L N_L)(M_R' - ik_R M_R)} . \tag{3.21}$$

Note that in the above equation for fermions, the factor (a_I/a_R) differs from unity, in contradistinction from the boson case. With the wave functions as given in Eqs. (3.12)–(3.15), we can obtain the incident, reflected, and transmitted currents as

$$\mathbf{J}_I = \frac{\mathbf{p}_I}{E} I^* I, \quad \mathbf{J}_R = \frac{\mathbf{p}_R}{E} R^* R, \quad \mathbf{J}_T = \frac{\mathbf{p}_T}{E'} T^* T . \tag{3.22}$$

For the problem of particle production probability under consideration, only the product T^*T and R^*R are involved. It is easy to show that these products have the same value when the function M is replaced by M^* and N is replaced by N^* in Eqs. (3.20) and (3.21). Thus, the transmission probability T^*T and reflection probability R^*R are the same for the cases of $\lambda = 1,2$ and the cases of $\lambda = 3,4$. Therefore, it is, in fact, not necessary to specify the quantum number η or the different λ states.

By a direct substitution of the special functions M and N and making use of the following properties[20] of the confluent hypergeometric function ${}_1F_1$:

$$\frac{d}{dx}{}_1F_1(\alpha,\gamma,x)=\frac{\alpha}{\gamma}{}_1F_1(\alpha+1,\gamma+1,x) ,$$

$$\left[1+\frac{x}{\gamma-1}\frac{d}{dx}\right]{}_1F_1(\alpha,\gamma,x)={}_1F_1(\alpha,\gamma-1,x) , \tag{3.23}$$

$${}_1F_1(\alpha,\gamma,x)=e^x{}_1F_1(\gamma-\alpha,\gamma,-x) ,$$

we can prove that

$$\left[\frac{d}{d\xi}-i\frac{\xi}{2}\right]M(a,\xi)=aN^*(a,\xi)$$

and (3.24)

$$\left[\frac{d}{d\xi}-i\frac{\xi}{2}\right]N(a,\xi)=M^*(a,\xi) .$$

We can then show from Eqs. (3.18)–(3.21) that

$$|R|^2=1-\left|\frac{k_RE}{k_LE'}\right||T|^2 . \tag{3.25}$$

This differs from the boson case in the sign of the term involving $|T|^2$. This expresses the expectation that for a fermion system, particles in a negative-energy state are reflected with an intensity smaller than the incident intensity, while for a boson system, a similar reflection of negative-energy states will give rise to a reflected wave with a greater intensity. This constitutes the so-called "Klein paradox" and corresponds to the possibility of particle-antiparticle creation in a strong field.[2,8,9]

We note again that the ratio $|k_RE/k_LE'|$ in Eq. (3.25) is equal to the ratio of the speed v_R of the particle in the z direction in region III to the speed v_L of the particle in the z direction in region I. From Eq. (3.22), we see that Eq. (3.25) expresses the conservation of current in the z direction: i.e.,

$$(\mathbf{J}_I+\mathbf{J}_R)\cdot\mathbf{e}_z=\mathbf{J}_T\cdot\mathbf{e}_z . \tag{3.26}$$

IV. PAIR-PRODUCTION PROBABILITY

The transmission amplitude is related to the probability of pair production.[2] We shall follow the derivation of Damour[2] to obtain such a relationship. With the potential of Fig. 1, it is possible to separate out incoming and outgoing states in the asymptotic regions as negative- and positive-energy states, depending on whether the energy is less than or greater than the asymptotic potential. These "negative" and "positive" energy states n_i and p_i form a complete basis in the asymptotic region. For our problem, we can take the incoming states as coming from the left (region I). The states satisfy the following orthonormality relations:

$$(p_i^{\rm in},p_j^{\rm in})=\delta_{ij}=\theta(n_i^{\rm in},n_j^{\rm in}) , \tag{4.1}$$

$$(p_i^{\rm in},n_j^{\rm in})=0 , \tag{4.2}$$

where the sign function θ is $+1$ for fermions, and, in accordance with the orthonormality condition (2.14), θ is -1 for bosons in a negative-energy state. We can expand the quantized field as

$$\Phi(x)=\sum_i[a_i^{\rm in}p_i^{\rm in}(x)+(b_i^{\rm in})^\dagger n_i^{\rm in}(x)] \tag{4.3}$$

with the commutator relations

$$[a_i^{\rm in},(a_j^{\rm in})^\dagger]_\pm=[b_i^{\rm in},(b_j^{\rm in})^\dagger]_\pm=\delta_{ij} , \tag{4.4}$$

where the anticommutators with the plus sign are for fermions and the commutators with the negative sign are for bosons. The "in" vacuum is defined by

$$a_i^{\rm in}\,|\,{\rm vac}^{\rm in}\rangle=b_j^{\rm in}\,|\,{\rm vac}^{\rm in}\rangle=0 . \tag{4.5}$$

We are interested in outgoing states in region III which also consist of positive- and negative-energy states. The outgoing states satisfy relations similar to those of Eqs. (4.1)–(4.5) and the field operator can be similarly expanded in terms of a complete set of outgoing positive- and negative-energy states in region III:

$$\Phi(x)=\sum_i[a_i^{\rm out}p_i^{\rm out}(x)+(b_i^{\rm out})^\dagger n_i^{\rm out}(x)] . \tag{4.6}$$

From the orthogonality conditions and Eqs. (4.1), (4.2), and (4.6), we get

$$a_i^{\rm out}=\sum_k[(p_i^{\rm out},p_k^{\rm in})a_k^{\rm in}+(p_i^{\rm out},n_k^{\rm in})(b_k^{\rm in})^\dagger] . \tag{4.7}$$

The phenomenon of particle creation consists of finding the outgoing positive-energy states in the "in" vacuum. The mean number of out particles in the out state $p_i^{\rm out}$ that is found in the "in" vacuum is given by

$$N_i=\langle\,{\rm vac}^{\rm in}\,|\,(a_i^{\rm out})^\dagger a_i^{\rm out}\,|\,{\rm vac}^{\rm in}\,\rangle . \tag{4.8}$$

Hence, from Eqs. (4.5) and (4.7), we have

$$N_i=\sum_k|(p_i^{\rm out},n_k^{\rm in})|^2 . \tag{4.9}$$

We can label the incoming state and the outgoing state by the energy E so that the $n^{\rm in}(E)$ tunnels only into the $p^{\rm out}(E)$ state with the same E. For example, in the boson case the incoming negative-energy state $n^{\rm in}(E)$ is represented by Eq. (2.12) and the outgoing positive-energy state $p^{\rm out}(E)$ by $\exp(ik_R\xi)$. In such a case, the number of positive-energy out particles created is

$$N(E)=|T(E)|^2 . \tag{4.10}$$

The ratio of the transmitted current of positive-energy particles to the incoming current is, therefore,

$$\frac{|\mathbf{J}_T|}{|\mathbf{J}_R|}=\frac{v_R}{v_L}|T(E)|^2 , \tag{4.11}$$

where the ratio of the speeds (positive quantities) v_R/v_I in region III and in region I is

$$\frac{v_R}{v_L}=\left|\frac{k_RE}{k_LE'}\right| .$$

In consequence, the rate of producing a positive-energy outgoing particle is, therefore,

$$\frac{\Delta N}{\Delta t}=\Delta x\Delta y\int\frac{p_z}{E}\frac{dp_zd\mathbf{p}_T}{(2\pi)^3}\frac{v_R}{v_L}|T(E)|^2 . \tag{4.12}$$

Thus, the quantity $(v_R/v_L)\,|\,T(E)\,|^2$ is proportional to the rate of production of a particle with energy E and transverse momentum $\mathbf{p}_T$ per unit time, unit transverse area, unit transverse momentum, and unit energy interval:

$$\frac{\Delta N}{\Delta t\,\Delta x\,\Delta y\,\Delta \mathbf{p}_T\,\Delta E}=\frac{1}{(2\pi)^3}\frac{v_R}{v_L}\,|\,T(E)\,|^2\,. \tag{4.13}$$

In this process of particle production due to the tunneling from the negative-energy state, a positive-energy particle is created, leaving a hole in the negative-energy continuum which can be taken to be an antiparticle moving in a direction opposite to the direction of the created particle. The created pair of particles is characterized by the energy E. For such a pair, one cannot, strictly speaking, specify a particular point as the location where the pair is produced, although this pair of particles begins to emerge at the points $z_L=(-E-m)/\kappa$ and $z_R=(-E+m)/\kappa$. Nevertheless, one can roughly associate the point $z=-E/\kappa$ as the location in the vicinity of which a pair of particles is produced. With this approximate association, the energy of the produced particle is then identified by an approximate location, and the energy interval also can be related (approximately) to a spatial interval at which the pair of particles is produced. From Eq. (4.13), the rate of production per unit volume and transverse momentum is then

$$\frac{\Delta N}{\Delta t\,\Delta x\,\Delta y\,\Delta z\,\Delta \mathbf{p}_T}=\frac{\kappa}{(2\pi)^3}\frac{v_R}{v_L}\,|\,T(E,\mathbf{p}_T)\,|^2\,. \tag{4.14}$$

Roughly speaking, the above results for the production probability and the production rate correspond to the lowest-order expansion in powers of $|\,T\,|^2$. One can obtain the higher-order corrections by studying the vacuum persistence probability. The vacuum persistence probability Q is the probability for finding the vacuum after the system has evolved over a period of time t and with a volume V containing the strong field. We can consider the initial vacuum as the state in which all the negative-energy states in region I are filled, so that there are no particles in the positive-energy states and no holes in the negative-energy states. For a single particle in a particular negative-energy state, this vacuum persistence probability has the same meaning as the reflection coefficient $|\,R\,|^2$ which is the probability of finding the outgoing negative-energy state in region I if a particle from the negative-energy state comes from the left. Taking into account all the different states with different spins z, t, and $\mathbf{p}_T$, the vacuum persistence probability is, therefore,

$$\begin{aligned}Q&=\prod_{\text{spin}}\prod_{z}\prod_{t}\prod_{\mathbf{p}_T}|\,R(z,\mathbf{p}_T)\,|^2\\&=\exp\left[\frac{\kappa}{8\pi^3}\int dV\,dt\,d\mathbf{p}_T\sum_{\text{spin}}\ln|\,R(z,\mathbf{p}_T)\,|^2\right].\end{aligned} \tag{4.15}$$

Because $|\,R\,|^2$ is greater than unity for bosons and less than unity for fermions [Eqs. (2.20) and (3.25)], the vacuum persistence probability is less than unity for fermions and greater than unity for bosons. This difference is due to particle production. From Eq. (4.15), we define the pair-production rate per unit volume, unit time, and unit transverse momentum $\mathbf{p}_T$ as

$$\frac{dN}{dV\,dt\,d\mathbf{p}_T}=-\frac{\kappa}{8\pi^3}\theta\sum_{\text{spin}}\ln\left[1-\theta\frac{v_R}{v_L}\,|\,T(E,\mathbf{p}_T)\,|^2\right]. \tag{4.16}$$

A comparison with the previous result of Eq. (4.14) shows that the more general result of Eq. (4.16) contains Eq. (4.14) as the lowest-order expansion. If one interprets $|\,T\,|^2$ as proportional to the probability of creating a single pair, then the result of Eq. (4.16) can be described as including additional effects of producing more than one pair.

We shall consider the limit of very large separation in order to compare our results with those of Schwinger. The transmission probability is an oscillating function of the energy (or correspondingly, the approximate location of pair production). It is also a function of the length of the separation L. We shall only consider the transmission probability at the midpoint between the two plates because the transmission probability at other locations is much more complicated. Using the asymptotic expression for the cylinder parabolic function $E(a,\xi)$ and the relation between $E(a,x)$ and $E(a,-\xi)$ (Ref. 20), [Eq. (19.18.3), (19.21.1), and (19.21.8) of Ref. 20], it is easy to show that when the separation L is very large, we can expand T in powers of $1/L$ and obtain for bosons the transmission probability at the middle between the plates:

$$\left|\frac{k_R E}{k_L E'}\right|\,|\,T\,|^2=e^{-2\pi a}\left[1+\frac{2}{\xi^2}(1+e^{-2\pi a})^{1/2}\sin 2\phi+O(\xi^{-4})\right], \tag{4.17}$$

where

$$\xi=|\,\xi_L\,|=\xi_R=\sqrt{\kappa/2}L$$

and

$$\phi=\frac{\xi^2}{4}-a\ln\xi+\tfrac{1}{2}\arg\Gamma(\tfrac{1}{2}+ia)+\frac{\pi}{4}\,.$$

For fermions, we need to expand the confluent hypergeometric function for large values of the argument ξ. Following the formulation of Ref. 25, we obtain the following expansion formula:

$$\begin{aligned}{}_1F_1(\alpha,\gamma,x)=&\frac{\Gamma(\gamma)}{\Gamma(\gamma-\alpha)}e^x\,|\,x\,|^{\alpha-\gamma}e^{-i(\alpha-\gamma)\pi/2}\\&\times\sum_{n=0}^{\infty}\frac{(-1)^n\Gamma(\gamma-\alpha+n)}{\Gamma(\alpha-n)n!}x^{-n}\\&+\frac{\Gamma(\gamma)}{\Gamma(\alpha)}\,|\,x\,|^{-\alpha}e^{-i\alpha\pi/2}\\&\times\sum_{n=0}^{\infty}\frac{\Gamma(\alpha+n)}{\Gamma(\gamma-\alpha-n)n!}x^{-n}\,.\end{aligned} \tag{4.18}$$

After considerable manipulation, we obtain the transmission probability at the midpoint between the plates as given by

$$\left|\frac{k_R E}{k_L E'}\right| |T|^2 = e^{-2\pi a}\left[1-\frac{\sqrt{2a}}{\xi^3}(1-e^{-2\pi a})^{1/2}\sin 2\phi + O(\xi^{-4})\right], \tag{4.19}$$

where

$$\phi=\frac{\xi^2}{4}-a\ln\xi+\tfrac{1}{2}\arg\Gamma(ia)-\frac{\pi}{8}\ .$$

Equation (4.17) for bosons and Eq. (4.18) for fermions give the corrections to the usual WKB result[3,5] of barrier penetration. We see that in both cases the transmission probability has a modulation due to the finite length of the separation. The magnitude of this modulation decreases as L increases. In the limit of $L\to\infty$, the transmission probability becomes $e^{-2\pi a}$, which is the WKB result. The reflection probability then becomes

$$|R|^2 = 1-\theta e^{-2\pi a} \tag{4.20}$$

and we have, for $L\to\infty$,

$$\frac{dN}{dV\,dt}=-\frac{\kappa}{8\pi^3}(2s+1)\theta \times\int_0^\infty d\mathbf{p}_T \ln\{1-\theta\exp[-\pi(m^2+\mathbf{p}_T^2)/\kappa]\}\ , \tag{4.21}$$

where s is the spin of the quanta under consideration. When we carry out the integration over $\mathbf{p}_T$ for this case, we obtain

$$\frac{dN}{dV\,dt}=\frac{\kappa^2}{8\pi^2}(2s+1)\sum_{n=1}\frac{(\theta)^{n-1}}{n^2}e^{-\pi n m^2/\kappa}\ , \tag{4.22}$$

where the sign θ is $+1$ for fermions and -1 for bosons. This result is identical to that of Schwinger,[1] and Brezin and Itzykson.[8] From Eq. (4.21), we can infer the pair-production rate per unit volume, unit time, and unit transverse momentum for the case of infinite spatial extension as

$$\frac{dN}{dV\,dt\,d\mathbf{p}_T}=-\frac{\kappa}{8\pi^3}(2s+1)\theta\ln(1-\theta e^{-2\pi a})\ . \tag{4.23}$$

This "Schwinger" result will be compared with the "exact" results of Eq. (4.16), using the transmission amplitude of Eqs. (2.16) and (3.18).

V. NUMERICAL EXAMPLES

It is useful to calculate the pair-production probability for a few cases of practical interest to see how the probability may depend on the finite size of the system involved. We shall examine the case of pair production when a quark q and an antiquark $\bar{q}$ are separated from each other by a distance L. Following Casher, Neuberger and Nussinov, we shall approximate the QCD problem by a problem in an Abelian gauge field in the same form as charged particles in a constant electric field between two parallel condenser plates in QED. The strength of the electric field is then related to the string tension of the "string" joining the quark and the antiquark. This string tension between q and $\bar{q}$, defined as the energy stored between the two particles per unit length, has been given previously by Casher, Neuberger, and Nussinov to be $\sigma=0.913$ GeV/fm, based on the Regge slope parameter. Using the flux-tube model and Gauss's law, we can relate this string tension constant σ to the potential parameter κ of the vector potential. The energy per unit length stored in the flux tube is related to the longitudinal field strength $\mathcal{E}$ and the cross-sectional area of the tube $\mathcal{A}$ by

$$\sigma=\tfrac{1}{2}\mathcal{E}^2\mathcal{A}\ . \tag{5.1}$$

Gauss's law relates the chromoelectric flux to the quark charge e:

$$\mathcal{E}\mathcal{A}=e\ . \tag{5.2}$$

From Eqs. (5.1)–(5.2), we obtain, therefore,

$$\kappa\equiv|e\mathcal{E}|=2\sigma=1.826\ \text{GeV/fm}\ .$$

This is the field strength κ for a static problem without particle production. However, as shown by Glendenning and Matsui,[5] when particles are produced, the final-state interaction between the quark q and the antiquark $\bar{q}$ of the produced $q\bar{q}$ pair will result in an effective string tension which is only half of the field strength for a string without particle production. This reduction is easy to understand. For a stretched quark and antiquark system represented by a string, a quark in the produced $q\bar{q}$ pair will interact only with the antiquark at the end of the string, while the interaction with the other quark at the other end is canceled by the final-state interaction with the newly produced quark. Hence, for numerical purposes, we shall use a string tension $\kappa=0.916$ GeV/fm and shall treat the quark as a massive particle with a mass[4] of $m=350$ MeV. With these parameters, the minimum length above which particles can be produced with $p_T=0$ is 0.78 fm.

We calculate numerically the production rate for both the bosons and the fermions with Eq. (4.16), using the transmission amplitude of Eqs. (2.16) and (3.18). The parabolic cylinder functions $E(a,\xi)$ and $E^*(a,\xi)$ are constructed with the formulas given in Ref. 20. For the confluent hypergeometric function ${}_1F_1(\alpha,\gamma,x)$ with small values of $|x|$, an expansion in powers of x is used.[20] However, for large values of L, it is necessary to use an expansion in power of $1/x$ as given by Eq. (4.18). As an independent check, we also numerically calculate the reflection probability R^*R and find that the relations of Eqs. (2.20) and (3.25) for T^*T and R^*R are satisfied to a high degree of accuracy.

We show in Figs. 2 and 3 the particle-production rate $dN/dV\,dt\,d\mathbf{p}_T$ (per unit time, unit volume, and unit transverse momentum) obtained as a function of the local coordinate $z'=z-L/2$, measured relative to the midpoint between the plates. As we remarked earlier, the location for the production of a pair cannot be sharply specified. What can be specified is the energy of the pro-

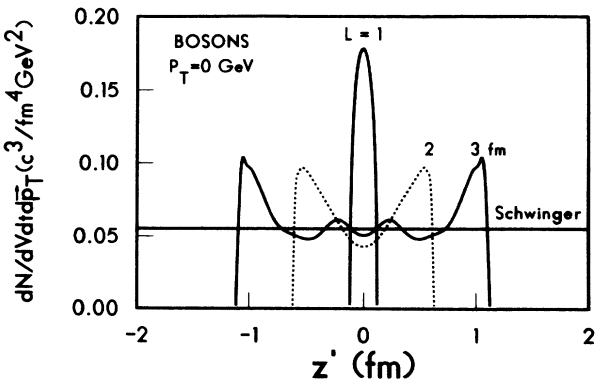

FIG. 2. We show here the particle-production rate (per unit volume, per unit time, and unit transverse momentum) for bosons when the plates are separated by $L=1$, 2, and 3 fm. The particle-production rate is plotted as a function of the location $z'=z-1/2$, which is measured relative to the midpoint between the plates. The strength of the field is set to be $\kappa=0.916$ GeV/fm and the mass of the boson is taken to be 0.350 GeV/c^2. For comparison, the Schwinger result deduced for an infinite system is shown as a horizontal line.

duced particles E which is related to the location by $E=-\kappa z$. When we refer to a location z (or z'), we should, therefore, associate this location with the corresponding energy. Figure 2 shows the "exact" results of the production rate for bosons obtained with Eqs. (2.16) and (4.16). The approximate "Schwinger" result of Eq. (4.22) is shown as the horizontal line. The rate of particle production is an oscillating function of the local coordinate. As the separation between the parallel plates increases, the rate at the midpoint between the plates comes quite close to the Schwinger result. The deviations from the Schwinger result are the greatest near the edges which are still some distance away from the plate. At the edges, the rate is about twice the Schwinger result. The spatial gaps between the edges of particle production and the location of the plates come about because there is a separation threshold for the occurrence of particle production. The potential difference needs to be as large as the sum of the rest masses of the produced particles for the process to take place. As the minimum separation for pair production is 0.78 fm, the case of $L=1$ fm has a separation just above the minimum distance for particle production. In that case, the deviation from the Schwinger result is large.

We show in Fig. 3 the "exact" particle-production rate for fermions $dN/dV\,dt\,d\mathbf{p}_T$ (per unit time, unit volume, and unit transverse momentum) as a function of the local coordinate z obtained from Eqs. (3.18) and (4.16). Again, the Schwinger result is also shown as a horizontal line. On the average, the rate of particle production for fermions is greater than that for bosons by a factor of 2 which arises from the spin degree of freedom. The rate of particle production as deduced from the Schwinger formula agrees approximately with that at the midpoint $z'=z-L/2\simeq 0$ for the case of $L=2$ and 3 fm, as it should be. However, for $L=1$ fm and in other regions of the coordinate, the production rate is quite different from the Schwinger result. For fermions, the deviation is of the order of 25% in different regions of the coordinate (Fig. 2). The deviation is, however, much greater for small separations near the threshold when the length of the separation is only slightly larger than the minimum length to allow the occurrence of particle production, as in the case of $L=1$ fm. For the same separation, the percentage of deviation from the Schwinger result is greater for the bosons than it is for the fermions.

To exhibit the dependence on the transverse momentum, we integrate the production rate $dN/dV\,dt\,d\mathbf{p}_T$ with respect to the thickness z from $z=0$ to $z=L$ and obtain $dN/dA\,dt\,d\mathbf{p}_T$ where dA is the transverse area element. In Fig. 4, we show the results for the production rate $dN/dA\,dt\,d\mathbf{p}_T$ (per unit time, unit area, and unit transverse momentum) as a function of the transverse momentum $|\mathbf{p}_T|$ for bosons. The dashed curves with open symbols are the Schwinger results obtained from Eq. (4.23) while the solid curves with solid symbols are "exact" results obtained with Eqs. (2.16) and (4.16). Curves with the diamond symbols are for the cases with $L=3$ fm, curves with the triangle symbols are for the cases of $L=2$ fm and curves with the square symbols are for the cases of $L=1$ fm. One observes that the Schwinger result and the "exact" result are proportional to each other for large values of the thickness ($L=3$ fm). In the semilogarithmic plot, the shapes of the two curves are similar to each other. The difference of the magnitude arises mainly from the fact that in the "exact" treatment, there is a region of the longitudinal coordinate for which particle production is not allowed. Hence, the Schwinger results are greater than the corresponding "exact" result. For small values of the thickness, the difference between the Schwinger result and the "exact" result is large.

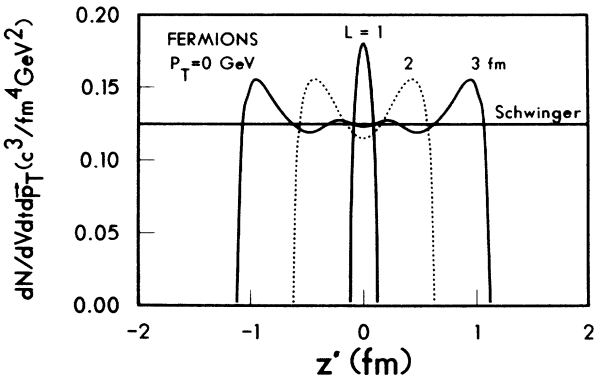

FIG. 3. We show here the particle-production rate $dN/dV\,dt\,d\mathbf{p}_T$ (per unit volume, per unit time, and unit transverse momentum) for fermions when the plates are separated by $L=1$, 2, and 3 fm. The particle production rate is plotted as a function of the location $z'=z-1/2$, which is measured relative to the midpoint between the plates. The strength of the field is set to be $\kappa=0.916$ GeV/fm, and the mass of the fermion is taken to be 0.350 GeV/c^2. For comparison, the Schwinger result deduced for an infinite system is shown as a horizontal line.

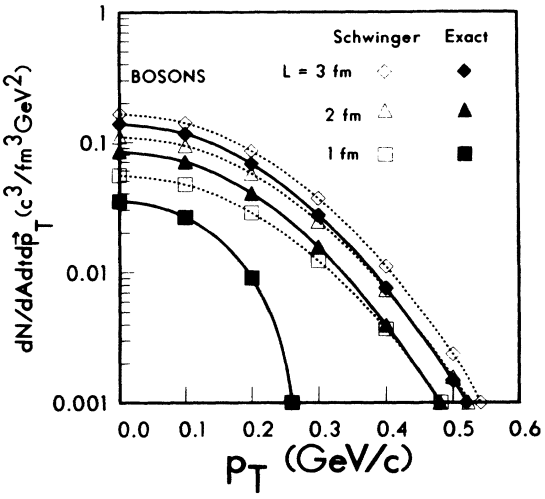

FIG. 4. We show here the particle-production rate $dN/dA\,dt\,d\mathbf{p}_T$ (per unit area, unit time, and unit transverse momentum) for bosons as a function of the transverse momentum $p_T=|\mathbf{p}_T|$, which is obtained by integrating $dN/dV\,dt\,d\mathbf{p}_T$ over the longitudinal coordinate z between the plates. The solid curves with the solid symbols are the "exact" results obtained from the present work and the dashed curves with the open symbols are the Schwinger results. To distinguish the different cases with different thicknesses of the strong field, we use the diamond symbols for the case of $L=3$ fm, triangle symbols for $L=2$ fm, and the square symbols for $L=1$ fm.

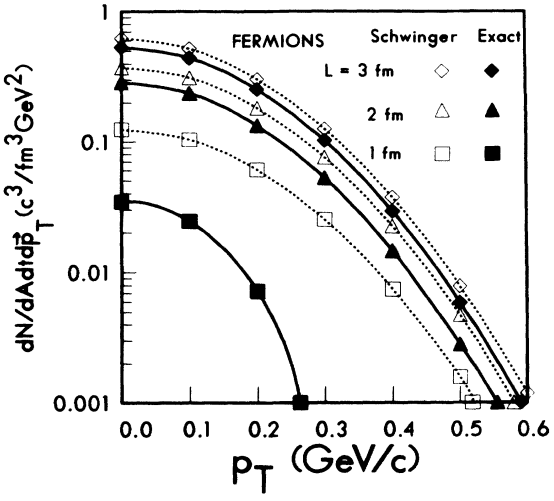

FIG. 5. We show here the particle-production rate $dN/dA\,dt\,d\mathbf{p}_T$ (per unit area, unit time, and unit transverse momentum) for fermions as a function of the transverse momentum $p_T=|\mathbf{p}_T|$, obtained by integrating $dN/dV\,dt\,d\mathbf{p}_T$ over the longitudinal thickness between the plates. The solid curves with the solid symbols are the "exact" results obtained from the present work and the dashed curves with the open symbols are the Schwinger results. To distinguish the different cases with different thicknesses of the strong field, we use the diamond symbols for the case of $L=3$ fm, triangle symbols for $L=2$ fm, and the square symbols for $L=1$ fm.

In Fig. 5, we likewise exhibit the dependence of the production rate on the transverse momentum for fermions by integrating the production rate $dN/dV\,dt\,d\mathbf{p}_T$ with respect to the thickness z from $z=0$ to $z=L$ and obtain $dN/dA\,dt\,d\mathbf{p}_T$ as a function of the transverse momentum $|\mathbf{p}_T|$. The dashed curves with open symbols are the Schwinger results obtained from Eq. (4.22) while the solid curves with solid symbols are "exact" results obtained with Eqs. (3.18) and (4.16). As in Fig. 4, curves with the diamond symbols are for the cases with $L=3$ fm, curves with the triangle symbols are for the cases of $L=2$ fm and curves with the square symbols are for the cases of $L=1$ fm. Again, one observes that the Schwinger result and the "exact" result are proportional to each other for large values of the thickness ($L=3$ fm). In the semilogarithmic plot, the shapes of the two curves are similar to each other. The difference of the magnitude arises mainly from the fact that in the "exact" treatment, there is a region of the longitudinal coordinate for which particle production is not allowed. Hence, the Schwinger results are greater than the corresponding "exact" results. For small values of the thickness, the difference between the Schwinger result and the "exact" result is again large.

Our comparison with the Schwinger result indicates that the Schwinger results for a uniform electric field of infinite extent give a good approximation to the particle-production rate in the central region between the plates when the separation between the plates is large. There are large deviations for other regions, especially at the edges of the production region, and when the separation threshold is just exceeded.

VI. CONCLUSIONS AND DISCUSSIONS

Starting from the Klein-Gordon equation and the Dirac equation, we have obtained the particle-production rate when the strong field is confined between two condenser plates separated by a finite distance. Our results complement those of Schwinger's which were obtained for an infinite system. The derivation presented here differs from the Green's-function approach of Schwinger but has the advantages of simplicity and the possibility of writing the results in simple closed forms. The production probability is obtained by solving exactly the Klein-Gordon or the Dirac equation, as the case may be, and matching the boundary conditions at the joining surfaces. The transmission probability is then extracted from the wave functions. We then relate the transmission probability to particle-production probability and obtain the production rate per unit volume, unit time, and unit transverse momentum. In the case of a boson field, the rate is given in terms of parabolic cylinder functions $E(a,x)$ and $E^*(a,x)$. In the case of the fermion field, it is written in terms of the confluent hypergeometric function ${}_1F_1$. We find that there is no production of particles until the separation between the plates exceeds a minimum threshold of $2mc^2/|e\mathcal{E}|$. When the separation is large, the production rates at the midpoint between the plate agree with the Schwinger results. However, there is a

finite-size effect which shows up for finite separations as large deviations from Schwinger's results for infinite systems. In particular, the deviations are large at the edges of the production zone. This edge effect is greater for the production of bosons than it is for the fermions. The deviations are also large when the separation between the plates exceeds just slightly the threshold separation for particle production. Thus, the Schwinger result is only a poor approximation when the separation is not large.

In view of various applications of the Schwinger particle-production mechanism, it will be of interest to see how the new results may be applied to particle-production processes in finite systems, such as in the decay of highly excited resonances, or to the production of particles in a strong Coulomb field, or ir e^+-e^- and nucleon-nucleon collisions. For these phenomena, the observable prediction of the present calculations are that (1) there is a threshold of the thickness of the strong field below which particles cannot be produced and (2) the energy spectrum of the produced particles has large variations due to the finite thickness of the strong field. The first consequence is a well-known result of the model. And, if we apply this result to high-energy collisions, one would expect that there is no particle production until the two sources producing the strong field have separated to a sufficient distance (above 1 fm). This feature agrees qualitatively with the experimental observation that particle production appears to occur at a time later than the instant at which a nucleon-nucleon collision takes place.[13,14] The second prediction of the present calculation has not yet confronted experimental tests. In lepton-hadron and e^+-e^- collisions, there is a recent proposal to measure the shape of an excited hadron by the use of the Bose-Einstein effect.[26] If this technique is found useful, then, it may be possible to correlate the energy spectrum of the produced particles with the longitudinal length of the decaying excited hadron and test the second prediction of the present calculation.

There are other interesting related problems which should be examined carefully if one wants to understand the particle production process in detail.[27] For example, the geometry of a flux tube has a finite extension in the transverse direction, while the present "condenser plate" problem is concerned with a transverse dimension which is infinite in extent. It would be of interest to see how a quantized motion in the transverse direction for a flux-tube geometry would affect the production rate. Another interesting problem is related to particle production in the collision of e^+ and e^- or in nucleon-nucleon collisions where the starting point of the production process involves a relative motion of the two quarks or the two leading particles. In contrast, the present study is static in nature. It will also be of interest to generalize the present study to examine particle production in systems where the two parallel plates are moving relative to each other. In the present analysis, the external field is idealized to be unaffected by the particle-production process. However, in reality, particle production will dissipate energy. If the strong field is generated by two leading particles, particle production will slow down the leading particles. To understand the so called "stopping of the leading particles,"[17,28–30] it will be useful to show how the production process is coupled to the dynamics of the leading particles so that the motion of the leading particles during the process of particle production can be followed.

ACKNOWLEDGMENTS

The authors wish to thank Professor P. Siemens and Professor C. M. Ko for helpful discussions, kind encouragement, and financial support without which this work would not have been completed. One of us (R.C.W.) wishes to thank the Nuclear Theory Group of Oak Ridge National Laboratory and Dr. J. B. McGrory for their kind hospitality. This research was supported in part by the Division of Nuclear Physics, U.S. Department of Energy under Contract No. DE-AC05-840R21400 with Martin Marietta Energy Systems, Inc. and in part by the National Science Foundation under Contract No. NSF 86-08149.

---

*Permanent address: Center of Astrophysics, China University of Science and Technology, Hofei, Anfei, China.

[1]J. Schwinger, Phys. Rev. **82**, 664 (1951).

[2]T. Damour, in *Proceedings of the First Marcel Grossmann Meeting on General Relativity,* edited by R. Ruffini (North-Holland, Amsterdam, 1977), p. 459; T. Damour and R. Ruffini, Phys. Rev. D **14**, 332 (1976); T. Damour, Helv. Phys. Acta **59**, 292 (1986).

[3]A. Casher, H. Neuberger, and S. Nussinov, Phys. Rev. D **20**, 179 (1979).

[4]A comprehensive review of the Lund model can be found in B. Andersson, G. Gustafson, G. Ingelman, and T. Sjöstrand, Phys. Rep. **97**, 31 (1983); other references on the Lund model include T. Sjöstrand, Comput. Phys. Commun. **39**, 347 (1986); B. Andersson *et al.*, Z. Phys. C **1**, 105 (1979); **20**, 317 (1983).

[5]N. K. Glendenning and T. Matsui, Phys. Rev. D **28**, 2890 (1983).

[6]Y. Srivastava and A. Widom, Phys. Lett. B **176**, 199 (1986); Phys. Rep. **148**, 1 (1987).

[7]C. Bottcher and M. R. Strayer, in *Physics of Strong Fields,* edited by W. Greiner (World Scientific, Singapore, 1987).

[8]E. Brezin and C. Itzykson, Phys. Rev. D **2**, 1191 (1970).

[9]H. Neuberger, Phys. Rev. D **20**, 2936 (1979); C. B. Chiu and S. Nussinov, *ibid.* **20**, 945 (1979).

[10]H. G. Dosch and D. Gromes, Phys. Rev. D **33**, 1378 (1986).

[11]P. H. Cox and A. Yidiz, Phys. Rev. D **32**, 819 (1985).

[12]S. W. Hawking, Commun. Math. Phys. **43**, 199 (1975).

[13]W. Busza, in *Proceedings of the 4th High Energy Heavy Ion Summer Study, 1978* (LBL Report No. 7766), p. 253.

[14]J. E. Elias *et al.*, Phys. Rev. Lett. **41**, 285 (1978); Phys. Rev. D **22**, 13 (1980).

[15]B. Andersson, G. Gustafson, and B. Nilsson-Almqvist, Nucl. Phys. **B281**, 289 (1987); B. Nilsson-Almqvist and E. Stenlund, Comput. Phys. Commun. **43**, 387 (1987).

[16]A. Capella and A. Krzywicki, Phys. Rev. D **18**, 3357 (1978); A. Capella and J. Tran Thanh Van, Z. Phys. C **10**, 249 (1981);

A. Capella, C. Pajares, and A. V. Ramallo, Nucl. Phys. **B241**, 75 (1984); A. Capella, A. Staar, and J. Tran Thanh Van, Phys. Rev. D **32**, 2933 (1985); A. Capella *et al.*, Z. Phys. C **33**, 541 (1987).

[17]C. Y. Wong, Phys. Rev. Lett. **52**, 1393 (1984); Phys. Rev. D **30**, 972 (1984); **32**, 94 (1985); Phys. Rev. C **33**, 1340 (1986).

[18]A. Bialas and W. Czyz, Nucl. Phys. **B267**, 242 (1986).

[19]T. Matsui, Nucl. Phys. **A461**, 27c (1987).

[20]M. Abramowitz and I. Stegun, *Handbook of Mathematical Functions* (Dover, New York, 1965).

[21]E. Ley Koo, Wang Renchuan, Ren Shangfeng, Sun Zongyang, and Hua Xinmin, J. China Univ. Sci. Tech. **13**, 167 (1983).

[22]C. Y. Wong and J. Bang, Phys. Lett. **29B**, 143 (1969).

[23]S. A. Fulling, Phys. Rev. D **14**, 1939 (1976).

[24]J. D. Bjørken and S. D. Drell, *Relativistic Quantum Fields* (McGraw-Hill, New York, 1965).

[25]P. M. Morse and H. Feshbach, *Method of Theoretical Physics* (McGraw-Hill, New York, 1953).

[26]L. S. Osborne, Phys. Rev. Lett. **60**, 987 (1988).

[27]C. Y. Wong, in *Lecture Notes for the 10th INS-Kikuchi Spring School on Quarks and Nuclei,* edited by O. Hashimoto and F. Sakata, 1977 (Institute for Nuclear Study, University of Tokyo, Tanashi, Tokyo, 1987), p. 178.

[28]W. Busza and A. S. Goldhaber, Phys. Lett. **139B**, 235 (1984).

[29]J. Kapusta, Phys. Rev. C **27**, 2037 (1983).

[30]M. Gyulassy, Phys. Rev. D **30**, 961 (1984).